# COMPARATIVE ASSESSMENT OF INTRACRANIAL ANEURYSMS USING 3D ROTATIONAL DSA AND 3T MRI: INITIAL EXPERIENCES

**IK Indrajit, C Mohan and K Pathak**

*Department of Radiodiagnosis, Army Hospital (Research and Referral) Delhi Cantt, New Delhi 110010, India*

***Abstract:*** *A pretreatment analysis of intracranial aneurysms by state of art imaging essentially entails accurate delineation of size and location of aneurysms, the aneurysm neck and its relation to parent and branch vessels. 3T MRI is a recently developed, costly, high-field imaging equipment, that is endowed with advantageous features such as high signal to noise ratio, easy applicability of increasing matrix size, superior background tissue suppression, the combination of which results in improved spatial resolution. This has enabled increased conspicuity of smaller intracranial vessels, with straightforward detection of small aneurysms.*

*This preliminary study analyzed the efficacy of 3T MR angiography on comparison with 3D rotational DSA, in assessment of ruptured and unruptured intracranial aneurysms, at our institute during the last six months. The study was performed in 6 patients with intracerebral aneurysms. The MRA data were examined as axial source data, MPR images of the source data, and MIP and 3D volume rendered images. Comparison were made with the 3D rotational DSA findings by analyzing aneurysm location, size, neck morphology, and branch vessel relationship to the aneurysm. Of the 6 aneurysms examined, 1 were small (,10 mm), two were large (10–25 mm), and two were giant (25 mm). One aneurysm was not detected with MRA, due to faulty technique of patient moving his head during the scan. 3D reconstructions of 3D rotational DSA and 3D reconstructions of 3T MRI in VR, were equal in accuracy. MPR images were particularly useful for defining branch vessels and the aneurysm neck. MRA is currently comparable to 3D rotational DSA in pretreatment assessment of intracranial aneurysms, and can miss lesions due toimproper technique.*

**Key Words**: Intracranial Aneurysms ; 3T MR angiography ; 3D rotational DSA

## INTRODUCTION

Pretreatment assessment is an important step in the management of patients presenting with features of intracranial aneurysms, for both aneurysm detection and surgical planning. Currently available imaging techniques include DSA, CTA, MRA and Transcranial Color Doppler[1]. Compared with the conventional DSA, rotational 3D-DSA can delineate intracranial vessels sharply[2] and intracranial aneurysms with greater levels of sensitivity and accuracy[3,4]. Since the first few studies in late 1980's, MR Angiography has emerged as an useful correlative neuroimaging modality to the gold standard DSA and is found increasingly useful in evaluation of intracranial aneurysm[5,6,7,8,9].

3T MRI is a recently developed, costly, high field imaging equipment, that is endowed with advantageous features such as high signal to noise ratio, easy applicability of increasing matrix size, superior background tissue suppression, the combination of which results in improved spatial resolution[10,11]. This has enabled increased conspicuity of smaller intracranial vessels, with straightforward detection of aneurysms with diameters even smaller than 2 mm and vessels smaller than 1 mm.[12] Further augmenting are post processing techniques, that offers multiple projections using MIP and SSD algorithm. MR image analysis comprises of axial source data, maximum intensity projection (MIP)[13] and shaded surface rendering. This study was designed to compare 3T MRA with 3D rotational DSA in the pretreatment assessment of both ruptured and unruptured cerebral aneurysms. The study was performed in patients with intracerebral aneurysms. MRA was analysed in the axial source data, multiplanar reconstruction (MPR), MIP and 3D SSD.

**Correspondence : Dr. I.K. Indrajit**, Consultant, Department of Radiodiagnosis, Army Hospital (Research and Referral) Delhi Cantt, New Delhi 110010, India **E-mail** : inji63@gmail.com

## MATERIAL AND METHODS

*Patients:* Six patients presenting with intracerebral aneurysms in a two month period were subject in the pretreatment assessment to 3T MRA and 3D Rotational DSA at our hospital. All patients in this study were subject to 3D Rotational DSA followed by 3T MRA a day later. The study group consisted of 4 female and 1 male; average age, 59 years). These patients presented either with aneurysmal subarachnoid hemorrhage (SAH) (n=5) or symptoms related to focal mass effect (n=1). The number of ruptured and unruptured cerebral aneurysms were five and one respectively. 4 patients were subject to elective clipping while two patients are under follow up.

## IMAGING MODALITIES AND ACUISITION

All intra-arterial DSA studies were performed on a Siemens 3D Rotational Biplane DSA system. Selective four vessel angiography using a standard projection format (anteroposterior, lateral, periorbital, and reverse-oblique) was performed initially with a femoral approach. Selective catheterization of the vessel harboring the aneurysm was performed by using a 5-F catheter. Three-dimensional DSA images were produced by a Workstation (Leoanrdo, Siemens Medical Systems) with the use of data from rotational

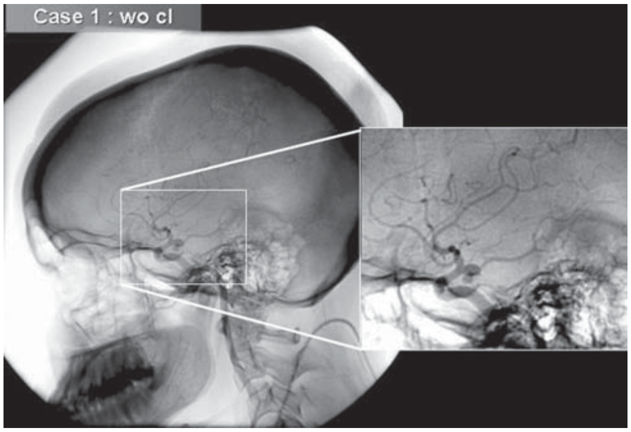


*Figure 1A: A 53 year-old woman presented with abrupt onset of headache and intractable pain. CT revealed subarachnoid hemorrhage. A diagnostic 3D rotational DSA showed a lobulated aneurysm located in the supraclinoid ICA*


*Figure 2A: A 50 year-old woman presented with mild headache, nausea and vomiting. CT revealed an unruptured aneurysm with no subarachnoid hemorrhage. She was assessed as Grade 4 SAH. A diagnostic 3D rotational DSA showed a small 2 mm sacular aneurysm in the junction of the callosomarginal and pericallosal of left anterior cerebral artery*

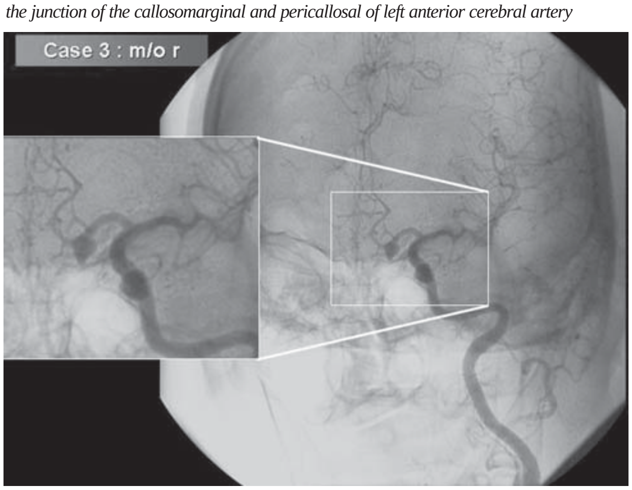


*Figure 3A: A 62 year-old woman presented with severe headache with loss of consciousness for 2 days. CT revealed subarachnoid hemorrhage. She was assessed as Grade 4 SAH. A diagnostic 3D rotational DSA showed a 7 mm aneurysm in the A1 segment of the anterior cerebral artery*


*Figure 1B: Thin Maximum intensity projection (MIP) reconstruction of MR angiogram (3D time-of-flight spoiled gradient-echo sequence, 24 msec /3.75 msec/ 1; TR/TE/NSA) shows a lobulated aneurysm located in the supraclinoid ICA*

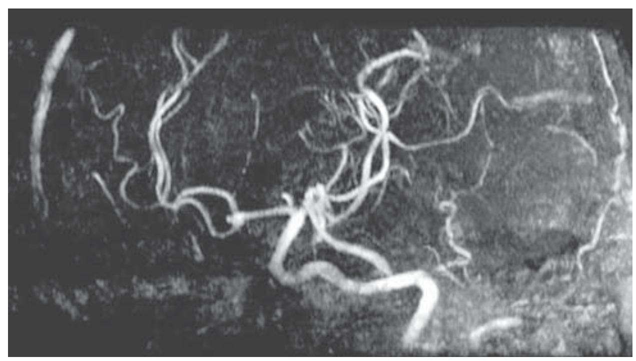

*Figure 2B: Maximum intensity projection (MIP) reconstruction of MR angiogram (3D time-of-flight spoiled gradient-echo sequence, 24 msec /3.75 msec/1; TR/TE/NSA) shows the a small 2 mm sacular aneurysm in the junction of the callosomarginal and pericallosal of left anterior cerebral artery. The relationship of the callosomarginal and pericallosal to the aneurysm can be clearly seen along its whole length.*

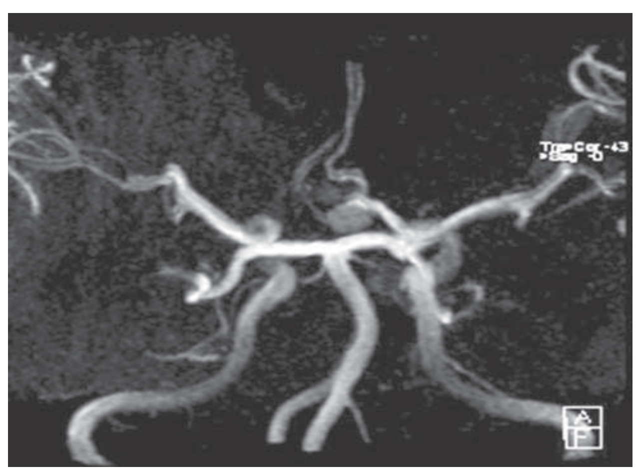

*Figure 3B: Maximum intensity projection (MIP) reconstruction of MR angiogram (3D time-of-flight spoiled gradient-echo sequence, 24 msec /3.75 msec/1; TR/TE/ NSA) shows the aneurysm in the A1 segment of the left anterior cerebral artery*

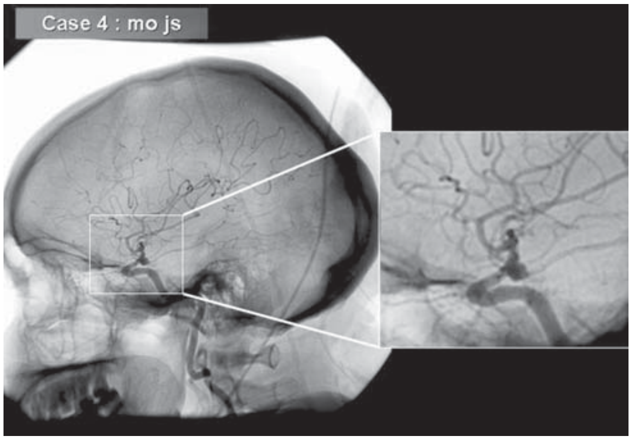


*Figure 4A: A 61 year-old woman presented with severe headache. CT revealed subarachnoid hemorrhage. She was assessed as Grade 2 SAH. A diagnostic 3D rotational DSA showed a 9 mm sacular aneurysm in the left posterior cerebral artery*

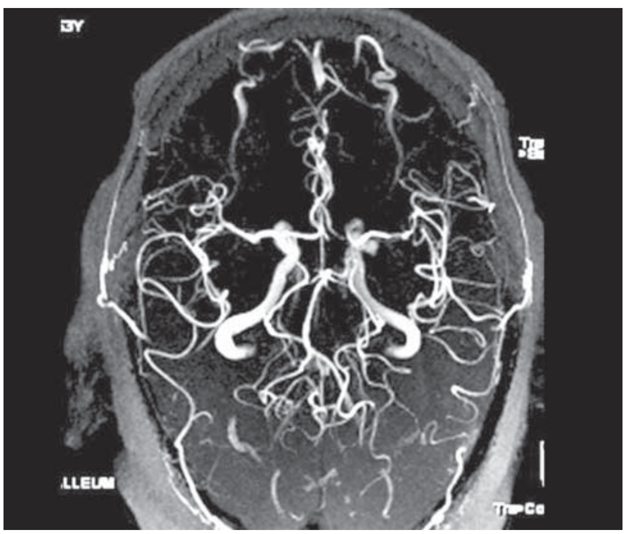

*Figure 4B: Maximum intensity projection (MIP) reconstruction of MR angiogram (3D time-of-flight spoiled gradient-echo sequence, 24 msec /3.75 msec/1; TR/TE/NSA) shows the sacular aneurysm in the left posterior cerebral artery The ipsilateral middle cerebral artery is of decreased caliber compared with the MIP-MRA projection.*

angiographies. Rotational angiography was performed with a 200° rotation of the C arm in 5 seconds. The matrix size of each frame was 512x512 pixels. Fifteen to 25 ml of the contrast medium (Iohexol, 300 mg/dl) was injected at a rate of 3 to 5 ml/s via a catheter positioned at the cervical portion of the carotid arteries and/or vertebral arteries. Both mask data and contrast data were automatically transferred to the workstation. 3D subtraction images were automatically produced on the workstation by a 3D-reconstruction algorithm based on the algebraic reconstruction technique. Reconstructed images, including MIP and shaded surface display were produced from the data. Minimum density threshold processing was automatically performed at the same levels. The maximum diameters of each aneurysm were calculated on the workstation.

MR examinations were performed on a 3-T Trio (Siemens) by use of a quadrature head coil. After a localizer scan was performed, 3D-TOF single-slab MRA acquisition (24/3.75/1; TR/TE/NSA); flip angle, 15; FOV, 22 cm; matrix, 512 x 512; slice thickness, 0.6 mm with 4 ot 5 slabs each comprising of 40 contiguous slices) was then performed through the circle of Willis, giving an effective voxel size of 0.6 x 0.3 x 0.6 mm. The acquisition time ranged from 8 to 9 minutes. Background tissue suppression was maximized by the addition of an off-resonance magnetization transfer gradient. An axial gradient spin-echo sequence (4500/110/4; FOV 22, cm; matrix, 256 x 256; echo train length, 8) through the brain was routinely performed in each case. The MR data were transferred to a Leonardo Syngo workstation for viewing and post processing.

## VIEWING AND POST PROCESSING

The 3D rotational DSA was reviewed first on the workstation monitor. MRA source images were displayed on the workstation, and MPRs were generated and viewed. Aneurysm size was assessed using MPR measurements along the maximum plane as well as MIP images that produced angiogram-like images. Three standard series of MIP reconstructions were produced, each consisting of 42 projections evenly spaced around a single rotational axis (foot-to-head, right-to-left, and front-to-back). Each aneurysm was rendered in multiple projections, with a comparable projection to the DSA projection. Thereafter SSD and VR were performed.

## POST PROCESSING OF IMAGES AND COMPARISON OF TECHNIQUES

Comparison of the visualization methods was retrospectively reviewed non-blinded by two senior radiologists. DSA findings and MR data (the source images, MPR, and MIP, 3D SSD, VR) were viewed to derive information on four key parameters: aneurysm detection, aneurysm shape and size morphology, neck and branch vessel characteristics. Measurements were made from the MPR data, with secondary measurement correlations taken form MIP images.

## TECHNIQUES AND RESULTS

On 3D rotational DSA, four aneurysms were in the distribution of the anterior communicating artery aneurysms, two were located in the middle cerebral artery. Of the 6 aneurysms examined with MRI, 1 were small (10 mm), two were large (10–25 mm), and two were giant (25 mm). One aneurysm showed minimal blurring from movement artifact due to faulty technique of patient moving his head during the MRI scan. In three cases, the aneurysm responsible for hemorrhage was surrounded by high-signal hematoma on MRI. Two patients subsequently underwent surgical clipping. Four aneurysms were not treated.

The majority of aneurysms were displayed well by all

**Table 1:** *Intracranial aneurysm : patient presentation and characteristics*

| S No | Pt Name | Age | Sex | Symptoms | Hunt and Hess clinical classification | Aneurysm Morphology on DSA: Location of Aneurysm | Size | Neck | Relationship with vessels | Treatment |
|---|---|---|---|---|---|---|---|---|---|---|
| 1 | w/o c lp | 44 | F | Abrupt onset of headache | Grade 1 | Origin of left posterior communicating artery | 8 x 5 mm Bilobed | Pointing posteriorly, inferiorly and medially | Vasospasm in proximal left posterior communicating artery | Intraoperative Clipping |
| 2 | w/o ms | 42 | F | Mild headache nausea and vomiting | Unruptured | Junction of callosomarginal and pericallosal of left ACA | 3.25 x 1.84 mm sacular aneurysm | Pointing anteriorly | ACA Normal | Conservative |
| 3 | m/o r | 73 | F | Severe headache Loss of consciousness | Grade 4 | Anterior communicating artery | 5.76 x 4.13 mm | Pointing inferiorly and medially | Filling of contralateral ACA via Anterior communicating artery | Intraoperative Clipping |
| 4 | m/o js | 53 | F | Severe headache | Grade 2 | Origin of left posterior communicating artery | 4.34 x 4.24 x 5.02 mm | Pointing posteriorly, and laterally | | Intraoperative Clipping |
| | | | | | | Distal part of M1 segment of MCA | 1.72 x 2.12 mm | Pointing posteriorly | Vasospasm of A1 and distal M2 segment | |
| 5 | BS | 45 | M | Headache Focal neurologic deficits | Grade 3 | Bifurcation of left MCA | 10x10x9 mm lobulated | Pointing anteriorly, superiorly and laterally | Vasospasm of MCA branches distal to aneurysm | Transorbital Clipping |
| 6 | m/o zh | 60 | F | Severe headache Meningismus | Grade 4 | Bifurcation of right MCA | 7 x 3 mm Lobulated | Pointing inferiorly and laterally | Haematoma lifting up branches of right MCA | Transorbital Clipping |

The Hunt and Hess clinical classification of SAH :
Grade 1 - Headache, slight nuchal rigidity
Grade 2 - Cranial nerve palsy, severe headache, nuchal rigidity
Grade 3 - Mild focal deficit, lethargy, confusion
Grade 4 - Stupor, moderate-to-severe hemiparesis, early decerebrate rigidity
Grade 5 - Deep coma, decerebrate rigidity, moribund appearance

techniques, including those shown by 3D rotational DSA. Interpretation was sequentially done, beginning from the axial source data, followed by MPR images and then reconstructed images. The smallest aneurysm detected by DSA and MRI was 2 mm. This aneurysm was located at junction of pericallosal and callosomarginal artery branching. None of the cases demonstrated intramural thrombus on MRI as hypointense crescentic area on MRI , or its correlates on the post processed 3D rotational DSA images. Measurements were made on source images or MPR images. The MPR, SSD and VR images were comparable to 3D rotational DSA images in all categories.

Regarding aneurysm detection MIP images were most suitable for aneurysm detection, including a 2mm aneurysm. As regards aneurysm morphology VR and SSD was better than MPR and MIP. Regarding aneurysm neck VR , SSD and MIP was better. Concerning branch relationship MIP delineated spasm more accurately than the surface rendered image. Regarding post processing techniques, the axial source data images were significantly inferior to 3D rotational DSA images. MPR was superior to MIP, excepting aneurysm detection. In the majority of cases, MRA images complemented 3D rotational DSA, without any significant add on information.

## DISCUSSION

Intracranial aneurysm is a common neurosurgical entity that is often asymptomatic until the time of its rupture. During rupture, the resultant subarachnoid hemorrhage rupture is a medical emergency and a potentially lethal event with a mortality rate as high as 50 percent[14]. Nearly 90 percent are saccular or berry aneurysms, which are responsible for most of the morbidity and mortality caused by subarachnoid hemorrhage[15].

Pretreatment assessment is an important step in the management of patients presenting with features of intracranial aneurysms, for both aneurysm detection and surgical planning. Intraarterial DSA has been traditionally considered the gold standard investigation modality for intracranial aneurysmal disease. It is an invasive technique with a 1% complication risk . Besides studies show that it has a 0.5% rate of persistent neurologic deficit[16,17].

One study compared the sensitivity and specificity of CTA, MRA and Transcranial Color Doppler for detecting intracranial aneurysms. While Magnetic resonance angiography has a sensitivity and specificity of 69 to 100 and 75 to 100%, the corresponding values for Computed tomographic angiography was 85 to 95 % and Transcranial Doppler ultrasonography was 50 to 91% and 87.5%[18]. A recent study analyzed the diagnostic accuracy of magnetic resonance angiography in correlation with 3D-digital subtraction angiographic images. 3D-TOF MRA was performed in 82 patients with 133 cerebral aneurysms. One hundred five (79%) of all 133 aneurysms were detected with MRA by a neuroradiologist, 100 (75%) were detected by an experienced neurosurgeon, 84 (63%) were detected by a general radiologist, and 80 (60%) were detected by a resident neuroradiologist. Evidently, the detectability was lower for small aneurysms (<3 mm in maximum diameter) and/or for those located at the internal carotid artery and anterior cerebral artery. False-positive diagnosis occurred due to complex flow in a tortuous artery and susceptibility artifacts[5]. MRA has been evaluated as a modality for the prospective detection of intracranial aneurysms[19].

Recently, Rotational 3-dimensional DSA (3D-DSA) has been increasingly used to obtain detailed information about the morphology and dimensions of intracranial aneurysms[19,20]. One such recent case analyzed the morphology of a patient presenting with a distal pericallosal artery aneurysm, revealed to be a saccular bifurcation aneurysm by 3D-DSA. The case report further highlights the value of 3D-DSA in establishing the appropriate treatment plan for patients with unique cerebral aneurysms. The authors rightly state that "accurate pre-interventional evaluation and differential diagnosis are critical to designing the most effective lowest risk treatment plan".[21]

The promise of evaluating aneurysms in 3D rotational DSA and 3T is slowly being realized across the world. To a large extent this is due to the fact that "recent neurointerventional and neurosurgical technologies require an understanding of lesions and adjacent structures in three dimensions"[22]. One study compared data of 52 patients treated before availability of 3D DSA with 33 patients treated after availability of 3D DSA (group B, 33 patients). The study showed that "3D DSA allowed acquisition of high-quality 3D images of cerebral arteries and also allows observation and analysis from multiple directions to determine the appropriate working projection for embolization"[22].

Another important aspect is "angiogram negative intracranial haemorrhage". This well established entity is encounterd in practice[23]. A study by Renowden SA evaluated 334 patients with DSA, of which no cause for haemorrhage could be identified in 41 (12%) cases. Of these 30 had predominantly subarachnoid (SAH) and 11 predominantly

**Table 2:** *Intracranial Aneurysm : Comparison Of Morphology*

| S No | Pt Name | Modality | Comparative Aneurysm Morphology on 3D Rotational DSA and 3T MRI | | | |
|---|---|---|---|---|---|---|
| | | | Location of Aneurysm | Size | Neck | Relationshi p with vessels |
| 1 | w/o c lp | 3D Rotational DSA | Origin of left posterior communicating artery | 8 x 5 mm Bilobed | Pointing posteriorly, inferiorly and medially | Vasospasm in proximal left posterior communicating artery |
| | | 3T MR A | At origin of left posterior communicating artery | 7.8 x 4.5 mm Irregular | Pointing posteriorly, inferiorly and medially | Normal calibre |
| 2 | w/o ms | 3D Rotational DSA | Junction of callosomarginal and pericallosal of left ACA | 3.25 x 1.84 mm sacular aneurysm | Pointing anteriorly | ACA Normal |
| | | 3T MR A | Junction of callosomarginal and pericallosal of left ACA | 3 x 1.7 sacular aneurysm | Pointing anteriorly | ACA Normal |
| 3 | m/o r | 3D Rotational DSA | Anterior communicating artery | 5.76 x 4.13 mm | Pointing inferiorly and medially | Filling of contralateral ACA via Anterior communicating artery |
| | | 3T MR A | Anterior communicating artery | 5.8 x 4.2 mm | Pointing inferiorly and medially | NA |
| 4 | m/o js | 3D Rotational DSA | Origin of left posterior communicating artery | 4.34 x 4.24 x 5.02 mm | Pointing posteriorly, and laterally | Normal calibre |
| | | 3T MR A | Origin of left posterior communicating artery | 4.3 x 4 x 5 mm | Pointing posteriorly, and laterally | Normal calibre |
| | | 3D Rotational DSA | Distal part of M1 segment of MCA | 1.72 x 2.12 mm | Pointing posteriorly | Vasospasm of A1 and distal M2 segment |
| | | 3T MR A | Distal part of M1 segment of MCA | 1.8 x 2.4 mm | Pointing posteriorly | Vasospasm of A1 segment |
| 5 | BS | 3D Rotational DSA | Bifurcation of left MCA | 10x10x9 mm lobulated | Pointing anteriorly, superiorly and laterally | Vasospasm of MCA branches distal to aneurysm |
| | | 3T MR A | Bifurcation of left MCA | 11x8x9 mm lobulated | Pointing anteriorly, superiorly and laterally | Vasospasm of MCA branches |
| 6 | m/o zh | 3D Rotational DSA | Bifurcation of right MCA | 7 x 3 mm Lobulated | Pointing inferiorly and laterally | |
| | | 3T MR A | Bifurcation of right MCA | 1 cm x 3 mm Lobulated | Pointing inferiorly and laterally | Haematoma lifting up branches of right MCA |

parenchymal haemorrhage (PH). An MRI was perfomed 1–6 weeks after the ictus, of which studies were positive in 7 patients (17%). In the 30 patients examined after SAH, 2 studies were positive, showing an aneurysm in one case and a brain stem lesion of uncertain actiology in the other. In those examined after PH, cavernous angiomas were shown in 2, a tumour in 1 and a vascular malformation in another; useful diagnostic information was thus obtained in 36% of this group of "angiogram negative intracranial haemorrhage" patients[23].

A study conducted at 8.0 T by Kangarlu and Shellock[24] reported that "all aneurysm clips, even those made from titanium or titanium alloy, displayed positive translational attractions (deflection angles ranged from 5 to 53 degrees). Importantly, several aneurysm clips reported to be safe at 1.5 T were found to be potentially unsafe at 8.0 T because they showed excessive deflection angles and relatively high qualitative torque values". The authors also recommend that at present, "aneurysm clips made from commercially pure titanium or titanium alloy are definitely safe because they exhibit no magnet-related movements in association with exposure to 3.0-T MR imaging systems. Aneurysm clips made from stainless steel alloy, Phynox, and Elgiloy, while displaying acceptable deflection angles (<45 degrees) and thus considered safe for patients and other persons in the long- and short-bore MR environments, require further characterization of torque effects to determine safety for patients who have these clips before allowing them to undergo MRI[25].

## CONCLUSION

Pretreatment assessment is an important step in the management of patients presenting with features of intracranial aneurysms, for both aneurysm detection and surgical planning. 3T MRI is a recently developed, costly, high field imaging equipment, that is endowed with advantageous features such as high signal to noise ratio, easy applicability of increasing matrix size, superior background tissue suppression, the combination of which results in improved spatial resolution. This has enabled increased conspicuity of smaller intracranial vessels, with straightforward detection of aneurysms with diameters even smaller than 2 mm and vessels smaller than 1 mm. 3T MRA is particularly useful in complex anatomic areas like middle cerebral artery bifurcation or anterior communicating artery. It is also useful in equivocal DSA studies in patients presenting with small aneurysms as also patients presenting with SAH with negative angiography.

## REFERENCES

1. *White PM, Wardlaw JM, Easton V. Can noninvasive imaging accurately depict intracranial aneurysms?: a systematic review. Radiology. 2000; 217: 361–370*
2. *Kang HS, Han MH, Kwon BJ, Kwon OK, Kim SH, and Chang KH, Evaluation of the Lenticulostriate Arteries with Rotational Angiography and 3D Reconstruction Am. J. Neuroradiol., 2005; 26(2): 306 - 312.*
3. *Unger B, Link J, Bohm-Jurkovic. Digital 3D-rotational angiography in preoperative and preinterventional diagnosis of intracranial aneurysms [in German]. Rofo Fortschr Geb Rontgenstr Neuen Bildgeb Verfahr. 1999; 170: 482–491*
4. *Tanoue S, Kiyosue H, Kenai H, Nakamura T, Yamashita M, Mori H. Three-dimensional reconstructed images after rotational angiography in the evaluation of intracranial aneurysms: surgical correlation. Neurosurgery. 2000; 47: 866–871*
5. *Okahara M, Kiyosue H, Yamashita M, Nagatomi H, Hata H, Saginoya T, Sagara Y, Mori H. Diagnostic accuracy of magnetic resonance angiography for cerebral aneurysms in correlation with 3D-digital subtraction angiographic images: a study of 133 aneurysms. Stroke. 2002;33(7):1803-8.*
6. *Anzalone N, Righi C, Simionato F, et al. Three-dimensional time-of-flight MR angiography in the evaluation of intracranial aneurysms treated with Guglielmi detachable coils. AJNR Am J Neuroradiol 2000; 21:746-752*
7. *Atlas SW, Sheppard L, Golberg HI, Hurst RW, Listerud J, Flamm E. Intracranial aneurysms: detection and characterization with MR angiography with use of an advanced postprocessing technique in a blinded-reader study. Radiology 1997; 203:807-814*
8. *Wilcock D, Japsan T, Holland I, Cherryman G, Worthington B. Comparison of magnetic resonance angiography with conventional angiography in the detection of intracranial aneurysms in patients presenting with subarachnoid haemorrhage. Clin Radiol. 1996; 51: 330–334*
9. *Masaryk TJ, Modic MT, Ross JS, Ruggieri PM, Laub GA, Lenz GW, Haacke EM, Selaman WR, Wiznitzer M, Harik SI. Intracranial circulation: preliminary clinical results with three-dimensional (volume) MR angiography. Radiology. 1989; 171: 793–799*
10. *Willinek WA, Gieseke J, von Falkenhausen M, Born M, Hadizadeh D, Manka C, Textor HJ, Schild HH, Kuhl CK. Sensitivity encoding (SENSE) for high spatial resolution time-of-flight MR angiography of the intracranial arteries at 3.0 T. Rofo. 2004;176(1):21-6.*
11. *Majoie C, Sprengers ME, van Rooij MJJ,Lavini C,Sluzewski M, van Rijn JC, den Heeten GJ. MR Angiography at 3T versus Digital Subtraction Angiography in the Follow-up of Intracranial Aneurysms Treated with Detachable Coils AJNR Am. J. Neuroradiol 2005; 26(6): 1349 - 1356.*
12. *Adams WM, Laitt RD, Jackson A. The Role of MR Angiography in the Pretreatment Assessment of Intracranial Aneurysms: A Comparative Study. Am J Neuroradiol 2000; 21:1618–1628*
13. *Anderson CM, Saloner D, Tsuruda JS, Shapeero LG, Lee RE. Artifacts in maximum-intensity-projection display of MR angiograms. AJNR Am J Neuroradiol 1990;154:623–629*
14. *Vega C, Kwoon JV, Lavine SD. Intracranial Aneurysms: Current Evidence and Clinical Practice. Am Fam Physician 2002;66:601-8.*
15. *Yong-Zhong G, van Alphen HA. Pathogenesis and histopathology of saccular aneurysms: review of the literature. Neurol Res 1990;12:249-55.*
16. *Heiserman JE, Dean BL, Hodak JA et al. Neurological complications of cerebral angiography. AJNR Am J Neuroradiol 1994; 15:1401–1407*
17. *Mayberg MR, Batjer HH, Dacey R, Diringer M, Haley EC, Heros RC, et al. Guidelines for the management of aneurysmal subarachnoid hemorrhage. A statement for healthcare professionals from a special writing group of the Stroke Council, American Heart Association. Stroke 1994;25:2315-28*
18. *Wardlaw JM, White PM. The detection and management of unruptured intracranial aneurysms. Brain 2000;123(pt 2):205-21*
19. *Hiraia T, Korogic Y, Suginoharab K, Onoa K, Nishia T . Clinical Usefulness of Unsubtracted 3D Digital Angiography Compared with Rotational Digital Angiography in the Pretreatment Evaluation of Intracranial Aneurysms. Am Jour Neuroradiology 2003; 24:1067-1074*
20. *Piotin M, Daghman B, Mounayer C, Spelle L, and Moret J. Ellipsoid Approximation versus 3D Rotational Angiography in the Volumetric Assessment of Intracranial Aneurysms Am. J. Neuroradiol 2006; 27(4): 839 - 842.*
21. *Woodworth GF, McGirt MJ, Clatterbuck R, Gailloud P. Evaluation of a distal pericallosal aneurysm visualized with 3-dimensional digital subtraction angiography: case report and treatment implications. Surg Neurol. 2005;64(4):321-4*
22. *Abe T, Hirohata M, Tanaka N, Uchiyama Y, Kojima K, Fujimoto K, Norbash AM, Hayabuchi N. Clinical benefits of rotational 3D angiography in endovascular treatment of ruptured cerebral aneurysm . AJNR Am J Neuroradiol. 2002 Apr;23(4):686-8.*
23. *Renowden SA, Molyneux AJ, Anslow P and Byrne JV. Diagnostic Neuroradiology. The value of MRI in angiogram-negative intracranial haemorrhage Neuroradiology 1994; 36: 6: 422 - 425*
24. *Kangarlu A, Shellock FG. Aneurysm clips: evaluation of magnetic field interactions with an 8.0 T MR system. J Magn Reson Imaging 2000;12:107–111*
25. *Shellock FG, Tkach JA, Ruggieri PM. Aneurysm Clips: Evaluation of Magnetic Field Interactions and Translational Attraction by Use of "Long-Bore" and "Short-Bore" 3.0-T MR Imaging Systems Am J Neuroradiol 2003; 24:463–471*